Activated Dynamics Across Aperiodic Stochastic Potentials†

Tricia D. Shepherd and Rigoberto Hernandez*

School of Chemistry and Biochemistry, Georgia Institute of Technology, Atlanta, Georgia 30332-0400

Received: March 5, 2002; In Final Form: May 21, 2002

In recent work, we have developed a new phenomenology allowing us to characterize the dynamics of particles on stochastic bistable surfaces well below the high-friction limit. [Shepherd, T. D.; Hernandez, R. *J.Chem.Phys.* **2001**, *115*, 2430.] A generalization of this class of bistable potentials to one-dimensional stochastic aperiodic potentials−viz. potentials which are not periodic in the sense that the barriers separating minima on a regular lattice are of unequal height−is pursued here. Several interesting aspects of the surface diffusion process across aperiodic stochastic potentials are compared to the well-established results for the periodic potential model. In particular, a suppression in the probability of correlated hops and an enhancement in the rate across aperiodic stochastic potentials are observed. Unique features characteristic of bistable stochastic potential models are also exhibited for this multi-barrier model. The most notable is the resonance enhancement of the escape rate (inverse escape time) which reaches a maximum at a nontrivial value of the barrier-correlation decay time.

I. Introduction

The motion of adatoms on metal surfaces has been of primary interest for some time because of the important role it plays in catalysis.[1−3] The experimental techniques of field ion microscopy and scanning tunneling microscopy also offer the possibility of probing the detailed dynamics.[4−11] Several stochastic models have been developed to describe this transport because the bulk, surface, and electronic modes are presumed to be weakly interacting with the diffusing adatoms.[1−3,6,12−28] Unfortunately, the disagreement between the various theories presently falls within the error bars of the experiment.[27] Nevertheless, the predominant conclusion is that surface diffusion can be modeled through the motion of particles undergoing activated dynamics across periodic potentials whose frequency matches that of the surface lattice, and the friction is far below the Smoluchowski regime.

An exciting new direction has recently been proposed by Pollak and co-workers,[26−28] in which they use their theory to suggest that the transport of the surface adatoms may be controlled via coherent external fields. In the present study, we investigate the possibility that dynamics across incoherent stochastic potentials−that have arisen either because some of the inherent modes are coupled to the system at longer time scales or because of external forces−may also give rise to spatially heterogeneous enhancements in the rates. If true, then this mechanism would provide an alternative with which to guide surface adatom transport.

In summary, the problem of describing the rate of an adatom across a surface is highly multidimensional with the dynamics resulting from the differing time scales of the bulk atoms, the surface atoms, the parallel and transverse motion of the adatoms, and electron reorganization. But these time scales are usually sufficiently separated that the equations of motion can be effectively decoupled through projection operator techniques leading to effective stochastic equations of motion. In particular, the surface and bulk atoms[1,2] as well as electron reorganization[3] readily project into this form through effective frictions that will not be distinguished in this work. The result is a three-dimensional stochastic equation of motion describing two modes parallel to the metal surface and a third mode transverse to the metal surface that exhibit rather different dynamics. The potential of mean force describing the parallel modes retains the periodicity of the lattice and perhaps even the aperiodicity of the lattice to the extent that there are small defects or surface deformations. The potential of mean force describing the transverse modes of captured (adsorbed) adatoms is presumably bounded at the temperatures of interest, and is often ignored. Meanwhile, the friction dissipating the parallel motion has been found to be in the low-friction regime presumably because the adatom interacts weakly with the metal surface.[19]

Thus, the problem reduces to the study of dynamics across essentially one-dimensional washboard potentials along a primary parallel mode. An approximate analytical solution of the escape rate for the one-dimensional periodic potential has been derived for the entire friction regime.[15,18] Such a transport can also be treated using a two-dimensional model in which the secondary parallel mode is bound as was studied by Pollak and co-workers in the case of time-independent potentials.[19] Instead, we restrict transport along the primary parallel mode, and focus on the dynamics that ensue when the potential of mean force is allowed to be time-dependent and represented as a stochastic aperiodic (incoherent) potential. The formalism for activated dynamics on stochastic aperiodic potentials is described in section II, and therein, the explicit forms of the potentials and simulation parameters are provided. The role of resonant activation in the dynamics as well as the purported rate enhancements are presented in section III.

II. Theory and Methods

The Langevin equation (LE) describing the dynamics of a Brownian particle in the presence of a stochastic potential is

$$\dot{v} = -\gamma v + \xi(t) + F_r(t), \tag{2.1}$$

† Part of the special issue "John C. Tully Festschrift".

* To whom correspondence should be addressed. E-mail: hernandez@chemistry.gatech.edu.

10.1021/jp020620h CCC: $22.00
Published on Web 07/12/2002

where $v(=\dot{x})$ is the velocity of the effective particle at the mass-weighted position x and γ is the friction constant. The time-dependent force $F_r(t)$ $[=-\partial U(x;t)/\partial x]$ depends on the time-dependent (stochastic) potential of mean force (PMF), $U(x;t)$. In the absence of a deterministic equation of motion for the PMF, it can be written as the sum of two terms, $U(x;t) \equiv \bar{U}_x + \delta U_t$, where $\bar{U}_x$ is the time-independent component corresponding to the time average of U at a fixed position x, and δU_t is the time-dependent component that is represented by a stochastic process that satisfies all known correlations in the deterministic δU_t. In the local limit that characterizes the LE, the short-time scale environmental response enters through the random forces $\xi(t)$−assumed to be Gaussian white noise with zero mean−maintaining thermal equilibrium through the fluctuation-dissipation relation (FDR),

$$\langle \xi(t)\xi(t')\rangle = 2k_B T\gamma_{th}\delta(t-t'), \tag{2.2}$$

where γ_{th} is the friction constant which thermalizes the system at the temperature T in the absence of any other noise terms. If all of the important fluctuations in the environment-induced force can be captured through the thermal fluctuations, $\xi(t)$, then $\delta U_t = 0$ and the LE is recovered with γ in eq 2.1 set to γ_{th} and $\xi(t)$ satisfying the FDR of eq 2.2. If, instead, the stochastic potential is nontrivial while maintaining thermal equilibrium, then it has recently been shown that the friction constant γ in eq 2.1 must be related to both thermal fluctuations in the LE and fluctuations in the stochastic potential.[29] In particular, the approximate renormalized friction constant, $\gamma^{(\infty)}$, can be constructed using a self-consistent (iterative) procedure. At each iteration, eq 2.1 is written as

$$\dot{v} = -\gamma^{(n)}v + \xi^{(n)}(t) + F^{(n)}(t), \tag{2.3}$$

where the friction $\gamma^{(n)}$ and random force $\xi^{(n)}$ satisfy the FDR at the n^{th} iteration, and the secondary noise term may be be written as

$$F^{(n)}(t) \equiv F_r(t) - [\xi^{(n)}(t) - \xi_{th}(t)]. \tag{2.4}$$

Treating $F^{(n)}(t)$ as if it were a local noise term leads to the expression,

$$\gamma^{(n+1)} = \gamma^{(n)}\left(\frac{\langle v^2(t)\rangle_n}{k_B T}\right), \tag{2.5}$$

where the average is taken with respect to $\gamma^{(n)}$. The error in this treatment is due to the existence of nontrivial cumulants in $F^{(\infty)}(t)$ at orders higher than the second order. In this sense, our treatment is mean-field like. In some cases, particularly in the overdamped regime, the friction requires effectively no correction as the contribution from the correlations in F_r is small compared to ξ_{th}.

For simplicity, the aperiodic stochastic potentials, $U(x;t)$, are modeled as a series of stochastic merged harmonic potentials (MHPs) of the form previously described in ref 29 for double-well potentials. Specifically, the potential is written as

$$U(x;t) \equiv U_m(x;t), \text{ for } m \text{ such that } x_m^0 < x \le x_{m+1}^0, \tag{2.6a}$$

where m labels the cell containing x, and the potential in the m^{th} interval for $k_m^{\ddagger} < k_0$ is defined as

$$U_m(x;t) = \begin{cases} \frac{1}{2}k_0(x - x_m^0)^2 & \text{for } x_m^0 < x \le x_m^- \\ V_m^{\ddagger} + \frac{1}{2}k_m^{\ddagger}(x - x_m^{\ddagger})^2 & \text{for } x_m^- < x \le x_m^+ \\ \frac{1}{2}k_0(x - x_{m+1}^0)^2 & \text{for } x_m^+ < x \le x_{m+1}^0, \end{cases} \tag{2.6b}$$

where the connection points are $x_m^{\pm} = \pm k_0\lambda/(2k_0 - 2k_m^{\ddagger}) + m\lambda$, and the end points are located at $x_m^0 = -\lambda/2 + m\lambda$ and $x_m^{\ddagger} = m\lambda$. (In practice, the probability of finding $k_m^{\ddagger}$ larger than k_0 has been so small that it has not occurred−vide infra. Nonetheless, in this limit, the form of U_m would be that of a bound well that must be matched to the potential of the neighboring intervals.) The force constant, $k_m^{\ddagger} \equiv -(k_0 + \eta(m,t))$ defines the barrier height $V_m^{\ddagger} = -k_0 k_m^{\ddagger}\lambda^2/(8k_0 - 8k_m^{\ddagger})$ and k_0 is a fixed parameter of the model. All energies and temperatures are reported in units of an arbitrary energy, $k_B T_0$, and arbitrary temperature, T_0, respectively.

Each barrier fluctuates independently according to the stochastic process $\eta(m,t)$. The parameters of the model are fixed such that the barrier height $V_m^{\ddagger}$ is 4 when η is 0. The average barrier height that results is only a few percent smaller than this value in the most extreme case.[29] Each $\eta(m,t)$ process is defined through an auxiliary Ornstein−Uhlenbeck process characterized by the probability distribution,

$$P(\eta) = \frac{1}{\sqrt{2\pi\sigma^2}}\exp\left\{-\frac{\eta^2}{2\sigma^2}\right\}, \tag{2.7}$$

and the time correlation,

$$\langle \eta(m,t)\eta(m,t')\rangle = \sigma^2\exp\left\{-\frac{|t-t'|}{\tau}\right\}, \tag{2.8}$$

where σ^2 is the variance related to the distribution of barrier heights and τ is the barrier-correlation decay time. Both values are taken to be independent of m throughout this work. For each $\eta(m,t)$, eq 2.8 is the well-known solution of an auxiliary stochastic equation,

$$\dot{\eta}(m,t) = -\frac{\eta(m,t)}{\tau} + \sqrt{\frac{2\sigma^2}{\tau}}\zeta(m,t), \tag{2.9}$$

where $\zeta(m,t)$ is a Gaussian white noise with correlation $\langle \zeta(m,t)\zeta(n,t')\rangle = \delta_{m,n}\delta(t-t')$. The coupled eqs 2.1 and 2.9 are propagated in time using the numerical integration method of Ermak and Buckholz.[30,31] Both positive and negative values of $k_m^{\ddagger}$ are possible because the value of ζ is sampled from a Gaussian distribution. The m^{th} cell will contain a maximum at $m\lambda$ for $k_m^{\ddagger} < 0$ and has the characteristic structure of two wells separated by a barrier. Otherwise, it will contain no maximum, and the overall structure is that of a single well when $\eta < -k_0$. There also exists a small probability that $x_m^+ > x_{m+1}^-$ resulting in a ill-defined potential when $\eta \le -2k_0$. The likelihood of these structures depends on the relative value of the variance, σ^2, as compared to the average of η, which is very small in the cases studied in this work. Figure 1 illustrates four realizations of the stochastic potential captured from an actual simulation at different times. It should be clear that the barriers are generally unequal at any given time and that their evolution is also independent of each other though they each retain some (fading) memory of their initial barrier height.

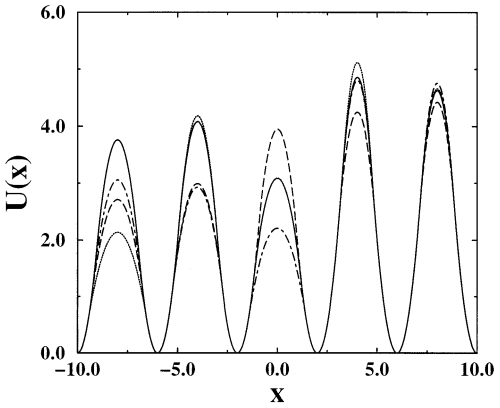

Figure 1. Four realizations of the aperiodic stochastic potential $U(x;t)$ are illustrated for a single trajectory at times (in units of τ): 0 (solid curve), 1/4 (dotted curve), 1 (dashed curve), 4 (dot-dashed curve). Each potential $U(x;t)$ is characterized by the same parameters, $-k_0 = 4$, $\lambda = 4$, and $\sigma^2 = 0.6$, and therefore has average barrier heights near 4. (The energies are reported implicitly in units of k_BT_0 for some standard temperature T_0, throughout).

The escape dynamics on this class of stochastic potentials is primarily characterized throughout this work using a rate set to the inverse mean-first passage time (MFPT). In the case of the LE over time-independent potentials, Hänggi and co-workers[32] have shown that the inverse MFPT is equivalent to the TST-like Kramers-Farkas flux-over-population rate. It has also been seen that more accurate inverse MFPT rates may be obtained by modifying the boundary surface with respect to which the first passage time is determined. In particular, we have recently obtained optimized escape rates across time-independent periodic potentials using a boundary surface defined in phase space.[33] Specifically, the first passage time, $\tau_{FPT}(i)$, for the i^{th} particle is the time it crosses the position $x \geq x^0_{m\neq 0}$ bounded by energy $E \leq k_BT$ in a particular unit cell $m(i)$. As was noted in earlier work,[33] once a particle has crossed this barrier it has effectively thermalized within the $m(i)$ unit cell, and we therefore refer to this as a *trapping event*. The MFPT is then defined as the average,

$$\tau_\Omega \equiv \lim_{N\to\infty} \frac{1}{N}\sum_{i=1}^{N} \tau_{FPT}(i), \qquad (2.10)$$

and the corresponding total rate Γ_∞ out of an initial well is the inverse MFPT, $1/\tau_\Omega$. Throughout this work, the MFPT was seen to converge with respect to both the minimum time step and the number of trajectories N, when they took on the values of 0.001 and 10 000, respectively. The critical conceptual point in the use of the MFPT for stochastic aperiodic potentials is that the expression, as written in eq 2.10, still holds despite that fact the barriers are now time-dependent and nonequal. It is unclear how a TST-like rate formula would be applied in this limit, and this manifests a present advantage of the MFPT approach.

III. Results and Discussion

A. Resonant Activation. The feature of the stochastic potential models that has primarily driven their study is the presense of a resonance phenomena in the escape rate, viz., an MFPT minimum is observed for a certain value of the barrier-correlation decay time, τ. This so-called "resonant activation" has been seen in a large number of bistable stochastic potential models with a wide range of friction spanning both the overdamped and underdamped regimes.[29,34−40,] Resonant activation is also a signature of aperiodic stochastic potentials for a wide range of friction as seen by the presence of minima in the MFPTs over the τ domain in Figures 2 and 3. (Note that the curves are displayed at fixed γ_{th} rather than fixed $\gamma^{(\infty)}$ because the latter contains a τ-dependent component.) Although not shown for brevity, the corrections $(\gamma^{(\infty)} - \gamma_{th})$ to the renormalized friction constant for the aperiodic stochastic potential were found to be essentially twice that of the corresponding correction for a bistable potential. This is presumed to result from the fact that the stochastic forces $F^{(\infty)}$ sample significant fluctuations at two essentially unconnected barrier regions in the former case whereas they sample only one barrier in the latter case.

A broad range of barrier correlation times were simulated in order to make comparisons at both the small and large τ limits

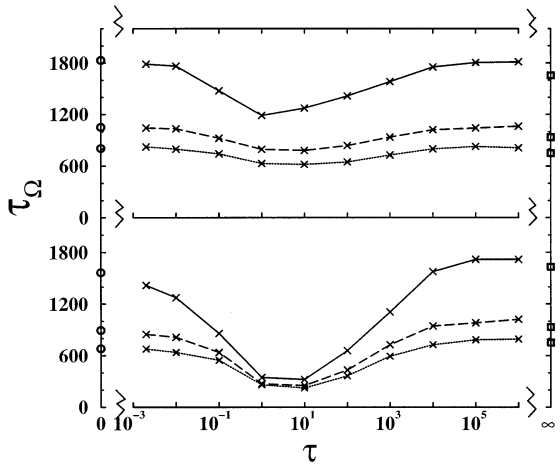

Figure 2. MFPT, τ_Ω, is displayed as a function of the correlation time, τ, at $k_BT = 2/3$ for several values of the friction constant γ_{th}: 0.08 (solid curve), 0.2 (dashed curve), and 0.4 (dotted curve). All simulations have been performed with the appropriate renormalized friction constant. The top and bottom panels are obtained for aperiodic stochastic potentials with variances, $\sigma^2 = 0.2$ and $\sigma^2 = 0.6$, respectively. The broken ordinate separates data obtained using direct simulations of the LE with stochastic potentials from the theoretically predicted limits at $\tau = 0$ and $\tau = \infty$. In the $\tau = 0$ limit, open circles represent numerical MFPT on the corresponding periodic potential with a fixed barrier height set to $\langle V^\ddagger \rangle$. In the $\tau = \infty$ limit, open squares correspond to the uncoupled barrier approximation in eq 3.2 using the numerical MFPT on a bistable MHP.

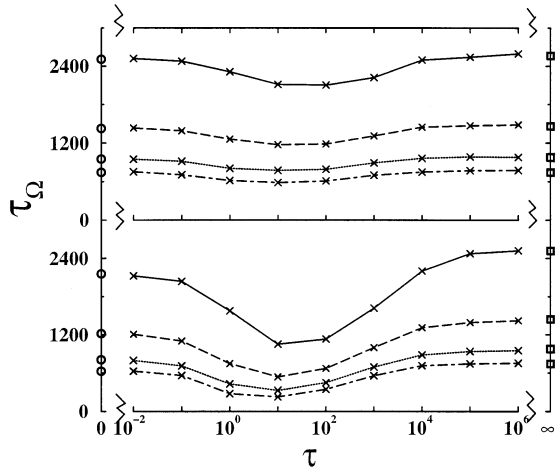

Figure 3. MFPT is displayed as a function of the correlation time, τ, in the overdamped regime at $k_BT = 2/3$ for several different values of the friction constant γ_{th}: 8 (solid curve), 4 (dashed curve), 2 (dotted curve), and 0.8 (dot-dashed curve). The remaining parameters are the same as in Figure 2 except analytic inverse rates are used to compute both the $\tau = 0$ and $\tau = \infty$ limits.

of this problem. As τ approaches the $\tau = 0$ limit for fixed variance σ^2, the system is reduced to a time-independent LE propagated by the average potential $\bar{U}_x$. This potential is consequently periodic with wells separated by barriers of equal height despite the fact that the stochastic potentials are aperiodic. As derived previously for bistable stochastic potentials,[29] the barrier height of $\bar{U}_x$ is the average of barrier heights, $\langle V^{\ddagger} \rangle$. The latter is determined with respect to the distribution of barrier heights,

$$P(V^{\ddagger}) = P(\eta(V^{\ddagger}))\frac{\partial \eta(V^{\ddagger})}{\partial V^{\ddagger}}. \tag{3.1}$$

For simplicity, we use the average barrier height to approximate $\bar{U}_x$ as a periodic MHP of the form of eq 2.6 with all the barrier heights set to $\langle V^{\ddagger} \rangle$, and suffer only a nominal error. At larger values of the friction, the inverse of the analytic rates across a periodic potential as given by Mel′nikov[15] are shown on the $\tau = 0$ axis of Figure 3. MFPTs from numerical simulations are plotted in Figure 2 because the analytic rates are not as accurate at small values of the friction unless finite-barrier corrections are taken into account.[41] Note that $k_B T = 2/3$ in all of these calculations, and consequently the average barriers are approximately six times the temperature. (The trends in the rates due to variations of the ratio between the temperature and the average barrier height have been explored earlier in the case of stochastic bistable potentials[29] but are not explored further in the present study.) At the wide range of friction explored in these simulations and for both sets of distributions, the low τ behavior of the MFPTs generally appear to be approaching their $\tau = 0$ limit. This agreement is suggestive of the validity of the $\tau \neq 0$ results.

In the opposite limit of slow barrier fluctuations (long barrier-correlation times), each particle is essentially propagated on a single realization of the aperiodic potential. The average rate is thus the average of the escape rates over each such realization. In cases when the escape dynamics out of the left and right exit channels are uncoupled, the rate for each realization of the stochastic potential can be approximated as the sum of the individual rates over each barrier. These in turn may be separately obtained using rate expressions for a double-well potential theory for the left and right barriers as characterized by the heights, $V_l^{\ddagger}$ and $V_r^{\ddagger}$, respectively. Because these two barrier heights are independently weighted by the probability $P(V^{\ddagger})$, the MFPT of the ensemble average is

$$\tau_{\Omega}(\infty) = \frac{\int_0^{\infty} dV_l^{\ddagger} P(V_l^{\ddagger}) \int_0^{\infty} dV_r^{\ddagger} P(V_r^{\ddagger}) \left(\frac{1}{\Gamma_0(V_l^{\ddagger}) + \Gamma_0(V_r^{\ddagger})} \right)}{\int_0^{\infty} dV_l^{\ddagger} P(V_l^{\ddagger}) \int_0^{\infty} dV_r^{\ddagger} P(V_r^{\ddagger})}, \tag{3.2}$$

where $\Gamma_0(V^{\ddagger})$ is the escape rate for a bistable potential with barrier height $V^{\ddagger}$. The solutions to this integral using Mel′nikov Meshkov rates[42] on a bistable MHP and numerical inverse MFPT rates are plotted on the $\tau = \infty$ axis of Figure 3 and Figure 2, respectively. The high τ behavior of the MFPTs generally appears to be approaching their $\tau = \infty$ limit suggesting that the $\tau \neq \infty$ results are consistent with this limit. The small deviations from this assessment seen in the low friction cases of Figure 2 likely result not from an error in the stochastic potential treatment but rather the fact that the approximation of uncoupled dynamics between adjoining barriers inherent in eq 3.2 breaks down. In this low friction limit, such an approximation leads to an underestimate of the MFPT, (overestimate of the rate), because it excludes trajectories that escape across one of the barriers after having first unsuccessfully explored the escape across the other barrier.

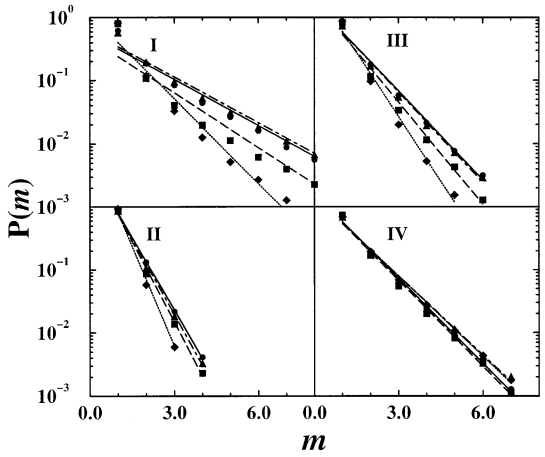

Figure 4. Correlated hopping probabilities, $P(m)$, are shown as a function of the jump length m from an initial well across the aperiodic stochastic potentials for several different values of the correlation time τ: 10^{-2} (diamonds and dotted line), 10^0 (triangles and dot-dashed line), 10^2 (squares and dashed line), and 10^5 (circles and solid line). Lines represent exponential fits though computed points. The first three panels correspond to the same variance, $\sigma^2 = 0.6$ but different friction constants: $\gamma_{th} = 0.08$ (I), $\gamma_{th} = 0.4$ (II), $\gamma_{th} = 0.2$ (III). Panel IV represents $\gamma_{th} = 0.2$ and $\sigma^2 = 0.2$.

B. Correlated Hopping Probabilities. In addition to the total escape rate, another figure of merit in the surface diffusion problem is the hopping probability distribution, $P(m)$. For moderate to small values of the friction, activated particles may cross more than one barrier before becoming retrapped in a potential well. These "correlated hops" have been observed in experiments[6,9] and in molecular dynamics simulations.[2,14,23,43] They have also been described using theoretical treatments of Langevin systems with time-independent periodic potentials.[17,18,21,26,44] In the present study, the jump length is determined by the absolute number of barriers $|m(i)|$ that the particle spans away from its initial escape upon first passage as described above eq 2.10. The hopping distribution, $P(m)$, is the probability a given particle will have a jump length $|m|$. In the overdamped friction regime only single hops with $m = 1$ are observed. Figure 4 displays $P(m)$ as a function of the jump length m for a variety of friction strengths γ_{th} and barrier correlation decay times τ. Panels I, II, and III provide the log of the hopping probabilities at three different values of the friction γ_{th}, respectively, for a distribution of stochastic MHPs with variance $\sigma^2 = 0.6$. The hopping probabilities displayed in panel IV are obtained at the same friction as in panel III but for a distribution with a smaller variance set to $\sigma^2 = 0.2$. As expected, the long-jump probabilities increase as the friction decreases. In addition, an exponential decay in the hopping distribution is observed at the larger friction values. This is to be expected when the escape processes are independent and the rate follows a simple first-order decay. As the friction decreases, significant deviations from exponential decay are evident at small values of m. Similar results have been observed with periodic potentials.[18,21,44]

Also apparent in Figure 4 is a significant dependence of the hopping distribution on the barrier correlation time, τ. The effect of τ on $P(m)$ increases with smaller frictions and larger variances. To show this τ dependence more clearly, Figure 5 displays the ratio $P_m(\tau)/P_m(0)$ of multiple hopping probabilities for a given τ as compared to the $\tau = 0$ limit described above.

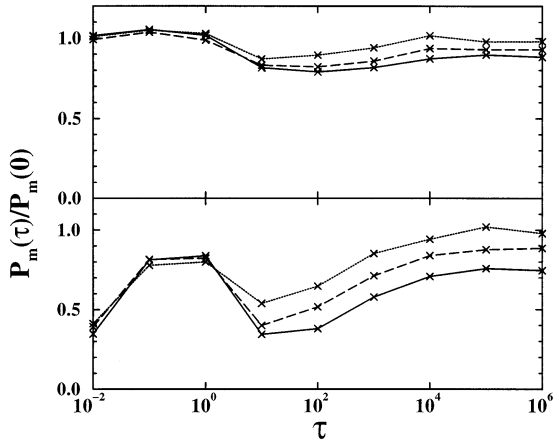

Figure 5. Multiple hop probabilities, $P_m(\tau) = 1 - P(1)$, for stochastic aperiodic potentials normalized by the results for the corresponding periodic potential with barrier height $\langle V^{\ddagger} \rangle$ are shown as a function of the barrier correlation time τ for several different values of the friction constant γ_{th}: 0.08 (solid curve), 0.2 (dashed curve), and 0.4 (dotted curve). The top and bottom panels are obtained for aperiodic stochastic potentials with variances, $\sigma^2 = 0.2$ and $\sigma^2 = 0.6$, respectively.

The multiple hopping probability across the stochastic aperiodic potential with $\tau \neq 0$ is defined as $P_m(\tau) \equiv 1 - P(1)$. (Note that the $\tau = 0$ limit of the stochastic aperiodic potential is a periodic potential and hence $P_m(0)$ is defined on such a surface.) In general, the multiple hopping probabilities for the aperiodic stochastic potentials are either comparable or suppressed in comparison to the periodic potential. Since each barrier fluctuates independently, it is possible that an activated particle will become trapped sooner if it encounters a significantly larger barrier along the aperiodic potential than it initially crossed when it escaped out of the initial basin of attraction. One might therefore expect to see reduced hopping suppression at smaller variances because of their correspondingly narrower distribution of barrier heights. This hypothesis is consistent with panels III and IV of Figure 4 and the two panels of Figure 5. Although not shown here, it is presumed that this effect may also diminish if some correlation between barriers is introduced.

In Figure 5, the bottom panel (corresponding to a larger variance) shows a significant suppression in the number of correlated hops at the smallest values of the barrier correlation time τ displayed. This, in turn, implies an enhancement of the single jumps in the aperiodic stochastic potentials which is as large as a factor of 2. For fast barrier fluctuations (small τ) correlated hopping will be suppressed because the probability of encountering a large second barrier is high due to the large number of barriers sampled during a crossing event. As τ increases, the probability of observing a high barrier will decrease and an increase in the correlated hopping rate is observed. Conversely, in the limit of slow barrier fluctuations (large τ) the aperiodic potential does not change significantly during a barrier crossing event. The heights of any two adjacent barriers will remain constant with values sampled according to eq 3.1. As τ decreases, the barrier heights will no longer remain fixed. Thus, there is an increasing probability of sampling a high second barrier leading to a suppression of the correlated hopping probability, P_m, as seen in Figure 5. As τ continues to decrease, eventually the system enters the regime near resonant activation. This in turn leads to a rise in the multiple hopping probability, P_m, because the system now effectively samples fewer high barriers due to significantly shorter escape times. Through this analysis, the predominant features of the results in Figure 5 are thus understood.

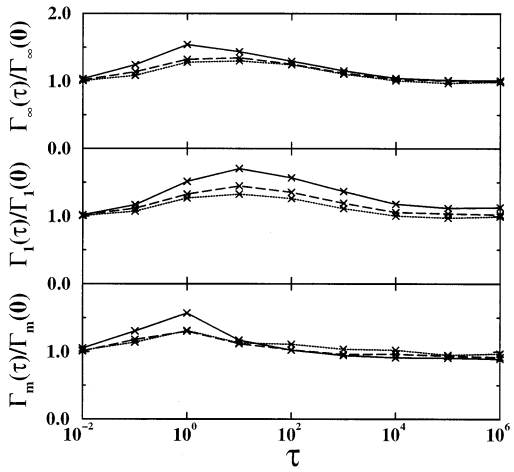

Figure 6. Hopping rates for stochastic aperiodic potentials normalized by the results for the corresponding periodic potential with barrier height $\langle V^{\ddagger} \rangle$ are shown as a function of the barrier correlation time τ for several different values of the friction constant γ_{th}: 0.08 (solid curve), 0.2 (dashed curve), and 0.4 (dotted curve). The three panels correspond to: the total multiple hopping rate Γ_∞ (I), the rate Γ_1 of single hops (II) and the cumulative rate Γ_m of multiple hops including all $m > 1$ (III). For all plots the value of the variance is $\sigma^2 = 0.2$.

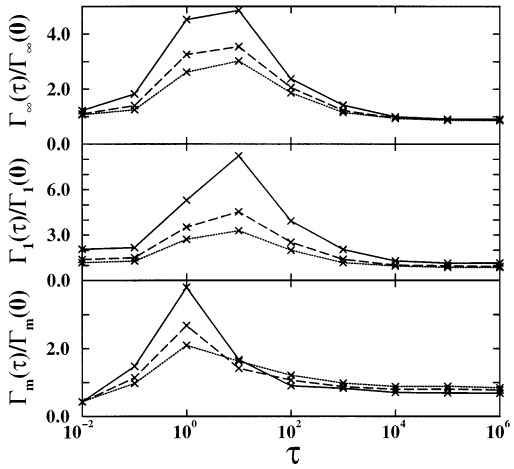

Figure 7. Normalized hopping rates as a function the barrier correlation time τ. All parameters are the same as Figure 6 except $\sigma^2 = 0.6$.

C. Rate Enhancement. While the hopping probabilities provide a general impression of the jump length across a surface, a more relevant quantity when considering surface dynamics is the actual time required to observe the multiple hops. The partial rate Γ_m is defined in terms of the overall jump rate such that $\Gamma_m = \Gamma_\infty P(m)$ and $P(m)$ is the probability of observing a jump of length $|m|$. By construction, the sum of all the individual rates equals the total rate. Three different characteristic hopping rates across the stochastic aperiodic potential are displayed in Figures 6 and 7 with each normalized by the corresponding fixed periodic potential with barrier height $\langle V^{\ddagger} \rangle$. The normalized total rate Γ_∞ [$=1/\tau_\Omega$], single hop rate Γ_1 [$=\Gamma_\infty P(1)$], and cumulative multiple hop rate Γ_m [$=\Gamma_\infty(1 - P(1))$], are shown in the top, middle, and bottom panels, respectively. Normalized rates are displayed in order to clearly show the magnitude of the rate enhancement with respect to the $\tau = 0$ limit. Again, it is clear that the surface dynamics may be significantly affected by both the variance and the barrier correlation time characterizing the aperiodic stochastic potentials.

Although an enhancement in the total rate, Γ_∞, is clearly visible in Figures 2 and 3, the top panels of Figures 6 and 7 illustrate the magnitude of the total rate enhancement relative

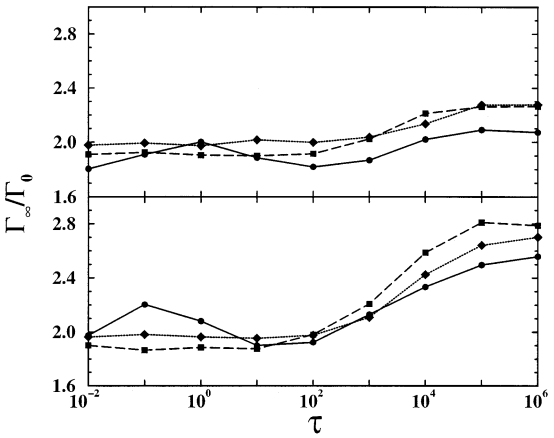

Figure 8. The ratio of the total rate Γ_∞ for aperiodic stochastic potentials to the rate Γ_0 for bistable stochastic potentials is shown as a function of τ for three values of the friction constant representing the underdamped ($\gamma_{th} = 0.08$ solid curve), turnover ($\gamma_{th} = 0.8$ dashed curve), and overdamped ($\gamma_{th} = 8.0$ dotted curve) regimes. The top and bottom panels are obtained for aperiodic stochastic potentials with variances, $\sigma^2 = 0.2$ and $\sigma^2 = 0.6$, respectively.

to the fixed periodic potential and is seen to be as large as a factor of 5 in the case of the larger variance ($\sigma^2 = 0.6$). If one is instead interested in the corresponding rate of single jumps Γ_1, then the rate enhancement peaks at close to nine times that of the periodic potential for intermediate values of the barrier correlation time, τ. The cumulative multiple hop rate enhancement is less significant, but it is noteworthy that the single hop rate and the multiple hopping rate peak at different values of the barrier correlation time.

A final interesting feature of this model is observed when the escape times of the aperiodic stochastic potentials are compared to results for the corresponding bistable stochastic potentials. It is generally understood that in the high friction (overdamped) regime, the presence of two equivalent exit channels in the periodic potentials leads to an escape rate that is twice that of a bistable potential. As the friction decreases, the possibility of correlated hops generally leads to a small suppression of this doubling because particles may revisit wells that they have already traversed.[33] However, the ratio of the rates, Γ_∞/Γ_0, for escape out of aperiodic and bistable stochastic potentials as a function of the barrier correlation time, τ, shown in Figure 8 actually exhibits rate enhancements. In particular, for moderate to large values of τ, an enhancement in the rate for the aperiodic stochastic potentials is observed regardless of the friction value. For a larger value of the variance ($\sigma^2 = 0.6$), this rate enhancement can be quite significant. It appears that for slower barrier fluctuations the particle can selectively "choose" to cross the smaller barrier thereby resulting in a faster escape rate.

IV. Concluding Remarks

Our recent developments in the use of activated dynamics with stochastic potentials below the high-friction limit make it possible to use these models for the first time on subsystems which are only weakly coupled to time-dependent environments. This is the case for the diffusion of adatoms on metal surfaces and as such our technique may add new insight into this problem. Moreover, because of the observed rate enhancements across one-dimensional stochastic aperiodic potentials, the use of our theory may also lead to the development of new experimental techniques to control the diffusion of the adatoms on the metal surface.

Acknowledgment. This work has been partially supported by a National Science Foundation CAREER Award under Grant No. NSF 97-03372. R.H.is a Cottrell Scholar of the Research Corporation and Alfred P. Sloan Fellow. The Center for Computational Science and Technology is supported through a Shared University Research (SUR) grant from IBM and Georgia Tech.

References and Notes

(1) Tully, J. C. *Annu. Rev. Phys. Chem.* **1980**, *31*, 319.
(2) Doll, J.; Voter, A. F. *Annu. Rev. Phys. Chem.* **1987**, *38*, 413.
(3) Tully, J. C. *Annu. Rev. Phys. Chem.* **2000**, *51*, 153.
(4) Ehrlich, G. *Appl. Phys. A* **1992**, *55*, 403.
(5) Kellogg, G. L. *Surf. Sci. Rep.* **1994**, *21*, 1.
(6) Senft, D. C.; Ehrlich, G. *Phys. Rev. Lett.* **1995**, *74*, 294.
(7) Swartzentruber, B. S. *Phys. Rev. Lett.* **1996**, *76*, 459.
(8) Zambelli, T.; Trost, J.; Wintterlin, J.; Ertl, G. *Phys. Rev. Lett.* **1996**, *76*, 795.
(9) Linderoth, T. R.; Horch, S.; Lægsgaard, E.; Stensgaard, I.; Besenbacher, F. *Phys. Rev. Lett.* **1997**, *78*, 4978.
(10) Pedersen, M. Ø.; Österlund, L.; Mortensen, J. J.; Mavrikakis, M.; Hansen, L. B.; Stensgaard, I.; Lægsgaard, E.; Nørskov, J. K.; Besenbacher, F. *Phys. Rev. Lett.* **2000**, *84*, 4898.
(11) Schunack, M.; Linderoth, T. R.; Rosei, F.; Lægsgaard, E.; Stensgaard, I.; Besenbacher, F. *Phys. Rev. Lett.* **2002**, *88*, 156 102.
(12) Tully, J. C. *J. Chem. Phys.* **1980**, *73*, 1975.
(13) Tully, J. C. *Surf. Sci.* **1982**, *111*, 461.
(14) Voter, A. F.; Doll, J. D. *J. Chem. Phys.* **1985**, *82*, 80.
(15) Mel′nikov, V. I. *Phys. Rep.* **1991**, *209*, 1.
(16) Dobbs, K.; Doren, D. *J. Chem. Phys.* **1992**, *97*, 3722.
(17) Ferrando, R.; Spadacini, R.; Tommei, G. E. *Phys. Rev. A* **1992**, *46*, R699.
(18) Pollak, E.; Bader, J.; Berne, B. J.; Talkner, P. *Phys. Rev. Lett.* **1993**, *70*, 3299.
(19) Gershinsky, G.; Georgievskii, Y.; Pollak, E.; Betz, G. *Surf. Sci.* **1996**, *365*, 159.
(20) Sholl, D. S.; Skodje, R. T. *Physica D* **1994**, *71*, 168.
(21) Jung, P.; Berne, B. J. In *New Trends in Kramers' Reaction Rate Theory*; Hänggi, P., Talkner, P., Eds.; Kluwer Academic: The Netherlands, 1995; pp 67−92.
(22) Georgievski, Y.; Kozhushner, M. A.; Pollak, E. *J. Chem. Phys.* **1995**, *102*, 6908.
(23) Jacobsen, J.; Jacobsen, K. W.; Sethna, J. P. *Phys. Rev. Lett.* **1997**, *79*, 2843.
(24) Caratti, G.; Ferrando, R.; Spadacini, R.; Tommei, G. E. *Phys. Rev. E* **1997**, *55*, 4810.
(25) Bao, J. D.; Abe, Y.; Zhuo, Y. Z. *Physica A* **1999**, *265*, 111.
(26) Georgievski, Y.; Pollak, E. *Surf. Sci. Lett.* **1996**, *355*, L366.
(27) Hershovitz, E.; Talkner, P.; Pollak, E.; Georgievski, Y. *Surf. Sci.* **1999**, *421*, 73.
(28) Talkner, P.; Hershkovitz, E.; Pollak, E.; Hänggi, P. *Surf. Sci.* **1999**, *437*, 198.
(29) Shepherd, T.; Hernandez, R. *J. Chem. Phys.* **2001**, *115*, 2430.
(30) Ermak, D. L.; Buckholz, H. *J. Comput. Phys.* **1980**, *35*, 169.
(31) Allen, M. P.; Tildesley, D. J. *Computer Simulations of Liquids*; Oxford: New York, 1987.
(32) Reimann, P.; Schmid, G. J.; Hänggi, P. *Phys. Rev. E* **1999**, *60*, R1.
(33) Shepherd, T.; Hernandez, R. *J. Chem. Phys.*, submitted.
(34) Doering, C. R.; Gadoua, J. C. *Phys. Rev. Lett.* **1992**, *69*, 2318.
(35) Hänggi, P. *Chem. Phys.* **1994**, *180*, 157.
(36) Reimann, P. *Phys. Rev. E* **1994**, *49*, 4938.
(37) Marchesoni, F.; Gammaitoni, L.; Menichella-Saetta, E.; Santucci, S. *Phys. Lett. A* **1995**, *201*, 275.
(38) Iwaniszewski, J. *Phys. Rev. E* **1996**, *54*, 3173.
(39) Reimann, P.; Hänggi, P. In *Stochastic Dynamics*; Schimansky-Geier, L., Poschel, T., Eds.; Vol. 484 of Lecture Notes in Physics; Springer: Berlin, 1997; pp 127−139.
(40) Boguna, M.; Porra, J. M.; Masoliver, J.; Lindenberg, K. *Phys. Rev. E* **1998**, *57*, 3990.
(41) Ferrando, R.; Spadacini, R.; Tommei, G. E.; Mel′nikov, V. I. *Phys. Rev. E* **1995**, *51*, R1645.
(42) Mel′nikov, V. I.; Meshkov, S. V. *J. Chem. Phys.* **1986**, *85*, 1018.
(43) Bader, J. S.; Berne, B. J.; Pollak, E. *J. Chem. Phys.* **1995**, *102*, 4037.
(44) Ferrando, R.; Spadacini, R.; Tommei, G. E. *Phys. Rev. E* **1993**, *48*, 2437.